ARTICLE

Mass Spectrometry Study of OH-initiated Photooxidation of Toluene

Ming-qiang Huang[a,b,c], Wei-jun Zhang[a,b*], Zhen-ya Wang[a,b], Li Fang[a,b], Rui-hong Kong[d], Xiao-bin Shan[d], Fu-yi Liu[d], Liu-si Sheng[d]

a. Key Laboratory of Atmospheric Composition and Optical Radiation, Anhui Institute of Optics and Fine Mechanics, Chinese Academy of Sciences, Hefei 230031, China
b. Laboratory of Environment Spectroscopy, Anhui Institute of Optics and Fine Mechanics, Chinese Academy Of Sciences, Hefei 230031, China
c. Department of Environmental Science and Engineering, Tan Kah Kee College, Xiamen University, Xiamen 363105, China
d. National Synchrotron Radiation Laboratory, University of Science and Technology of China, Hefei 230029, China

(Dated: Received on June 30, 2011; Accepted on August 5, 2011)

The composition of products formed from photooxidation of the aromatic hydrocarbon toluene was investigated. The OH-initiated photooxidation experiments were conducted by irradiating toluene/CH_3ONO/NO/air mixtures in a smog chamber, the gaseous products were detected under the supersonic beam conditions by utilizing vacuum ultraviolet photoionization mass spectrometer using synchrotron radiation in real-time. And an aerosol time-of-flight mass spectrometer was used to provide on-line measurements of the individual secondary organic aerosol particle resulting from irradiating toluene. The experimental results demonstrated that there were some differences between the gaseous products and that of particle-phase, the products of glyoxal, 2-hydroxyl-3-oxo-butanal, nitrotoluene, and methyl-nitrophenol only existed in the particle-phase. However, furane, methylglyoxal, 2-methylfurane, benzaldehyde, cresol, and benzoic acid were the predominant photooxidation products in both the gas phase and particle phase.

Key words: Toluene, Secondary organic aerosol, Smog chamber, Desorption/ionization, Reaction mechanism

I. INTRODUCTION

The high levels of monocyclic aromatic compounds in urban areas is directly linked to anthropogenic activity such as fossil burning and solvent use [1−3]. The importance of the contribution of aromatic hydrocarbons to the problems of urban air pollution is well established today. Besides their carcinogenic and mutagenic effects on living organisms and human health, in the presence of NO_x, the degradation of these compounds in the troposphere contributes substantially to the ozone and photooxidant burden and also the formation of secondary organic aerosol (SOA) [4−7], which are known to be harmful to human and ecosystem health [8−10]. As emissions of aromatic hydrocarbons are concentrated in urban areas, where many people live and work, the formation of SOA becomes a more acute problem [11].

Of the aromatics, benzene, toluene, xylene, ethylbenzene, and 1,2,4-trimethyl-benzene make up 60%−70% of this load, with toluene being one of the most significant compounds [7]. In the past decade, the studies on reaction mechanism and degradation products of photooxidation of toluene are of particular interest [6, 7, 12, 13]. The gas phase products are collected using cryogenic trapping system or solid phase adsorbent tubes, then samples were flash heated and injected onto the head of the gas chromatograph column. The SOA particles formed from the photooxidation of toluene were usually collected using filters or impactor plates and samples were prepared by the way of chemical extracts. Molecular composition of SOA particles could be analyzed by gas chromatograph/mass spectrometer (GC/MS) [13]. However, there are some disadvantages in GC/MS, for example, possible secondary chemical reactions or loss of semivolatile compounds associated with traditional aerosol sampling onto a filter or impactor plate, or with multi-step chemical treatments.

From the mid 1990s, real-time laser mass spectrometry has been remarkably developed, offering new opportunities for on-line studying gaseous and particulate matters [14]. However, for the high laser intensity required to desorb and ionize the gaseous products, organic ions generated will readily absorb multiple UV photons resulting in massive fragmentation [15]. So for gaseous products, new "soft" ionization methods are

*Author to whom correspondence should be addressed. E-mail: wjzhang@aiofm.ac.cn

needed to minimize the fragmentation in the mass spectra. As we all know, synchrotron radiation provides vacuum ultraviolet light and soft X-rays which are used for a wide range of analytical techniques [16, 17]. To the best of our knowledge, no investigations on detecting the toluene photooxidation gaseous products using synchrotron radiation are performed up to now. Our laboratory has demonstrated that aerosol time-of-flight mass spectrometry (ATOFMS) can be used to measure the size and chemical composition of particles in real-time [18].

In this work, the photooxidation of toluene was initiated by hydroxyl radical (OH·) in a home-made smog chamber, vacuum ultraviolet photoionization mass spectrometer (PIMS) using synchrotron radiation and ATOFMS was employed to detect the gas-phase products and the individual particles in real-time respectively.

II. EXPERIMENTS

A. Vacuum ultraviolet photoionzation mass spectrometry

Our experimental apparatus has been described previously elsewhere [19, 20]. In brief, we performed vacuum ultraviolet photoionzation mass spectrometry (VUV-PIMS) measurements on the atomic and molecular physics beamline with the supersonic expansion molecular beam/a reflectron time-of-flight mass spectrometer (RTOFMS) system at National Synchrotron Radiation in Hefei, China. Photon energies in the region of 7.5−22.5 eV with a resolving power of 5000 at 15.9 eV and a photon flux of 10^{12} photon/s were selected with a grazing-incidence SGM monochromator employing a grating of 370 grooves/mm and a slit width of 80 μm. The gaseous sample was introduced by a supersonic expansion through a continuous beam nozzle with an orifice of 70 μm diameter from the molecular beam chamber into the differential chamber through a 1 mm skimmer. A secondary skimmer collimates the molecular beam to enter the ionization chamber where the sample molecular beam intersected the monochromatized synchrotron radiation beam at 70 mm from the nozzle. A RTOFMS was employed for the VUV photoionization/fragmentation studies. The ions were taken out of the photoionization region by a pulse extraction field triggered with a pulse generator (DG 535 SRS) and detected by a microchannel plate (MCP) detector. The ion signal was recorded by a multiscaler P7888 (FAST Comtec, Germany) after it was amplified with preamplifier VT120C (EG&G, ORTEC).

B. Aerosol time-of-flight mass Spectrometer

ATOFMS is a home made single particle mass spectrometer, which is designed to measure individual aerosol particles in real time [13, 18]. Particles are introduced into the instrument through a converging nozzle. The nozzle is separated from a skimmer and the region is mechanically pumped to a pressure of ∼266 Pa. The expansion of molecules in this region accelerates the particles to velocities dependent on their aerodynamic size. A secondary skimmer allows for differential pumping to reach the pressures needed to operate the mass spectrometer and collimates the particle beam by removing particles that do not follow a straight trajectory through the nozzle. Particles then enter a light scattering region where they encounter two green continuous-wave, diode-pumped lasers separated by a known distance. The lasers are positioned perpendicularly to one another and orthogonally to the particle beam. For each laser, an arrangement of optics is used to focus the laser beam to a spot that intersects the particle beam. A particle passing through each laser beam scatters light which is collected by an ellipsoidal mirror and focused onto a photomultiplier tube (PMT) detector. The PMTs send pulses to an electronic timing circuit that measures the time required for the particle to travel the known distance between the two scattering lasers [13, 18]. The distance and the particle time-of-flight are used to calculate the particle velocity. An external size calibration uses particles of known size to relate the velocity to a physical aerodynamic diameter. Once the circuit begins a countdown to the time when the particle will reach the center of the ion source region of a mass spectrometer. At this time, the circuit sends a signal to a fire a pulsed excimer KrF laser at 248 nm having an average power density of $\sim 10^6$ W/cm^2 and a pulse length of 2.5 ns. Upon absorption of the laser pulses, the particle is heated in a rapid fashion, desorbing and ioning individual molecules from the particle. The resulting positive ions are mass analyzed in a linear time-of-flight mass spectrometer. For each particle analyzed, the size is obtained through the particle velocity and the corresponding particle composition is determined through the positive ion mass spectra.

C. Smog chamber experiment

Toluene (>99%) was obtained from Sigma-Aldrich Chemistry Corporation, Germany. Sodium nitrate (>99%) and methanol (>99%) were purchased from the Tianjin (The third Reagent Manufactory), and nitrogen oxide (99.9%) from Nanjing Special Gas Factory.

Methyl nitrite was synthesized by dropping sulfuric acid into a methanol solution of sodium nitrate. Their reaction products passed through saturated sodium hydroxide trap to remove the traces of sulfuric acid, and were dried by passing through a calcium sulfate trap and collected using a condenser of liquid nitrogen at 77 K. The methyl nitrite was purified using a vacuum system of glass.

Photooxidation of toluene was performed using UV-

DOI:10.1088/1674-0068/24/06/672-678

irradiation of toluene/CH_3ONO/NO/air mixtures in our home-made smog chamber [13, 18]. Prior to starting each experiment, the chamber was continuously flushed with purified laboratory compressed air for 20 min, and evaluated to a vacuum of 0.1 Pa by a mechanical pump. The compressed air was processed through three consecutive packed-bed scrubbers containing, in order, activated charcoal, silica gel and a Balston DFU® filter (Grade BX) respectively, to remove the trace of hydrocarbon compounds, moisture and particles. Toluene was sampled by a micro liter injector and injected directly into the chamber. NO and methyl nitrate were expanded into the evacuated manifold to the desired pressure through Teflon lines, and introduced into the smog chamber by a stream of purified air. The whole system was completely shrouded from light with a black polyethylene tarpaulin. Hydroxyl radicals were generated by the photolysis of methyl nitrite in air at wavelength longer than 300 nm [21]. The chemical reactions leading to the formation of the OH· radical are:

$$CH_3ONO \xrightarrow{h\nu(300\ \text{nm})} CH_3O\cdot + NO\cdot \quad (1)$$

$$CH_3O\cdot + O_2 \rightarrow HCHO + HO_2\cdot \quad (2)$$

$$HO_2\cdot + NO\cdot \rightarrow OH\cdot + NO_2\cdot \quad (3)$$

The initial concentration of toluene, CH_3ONO and NO was 10, 100, and 20 ppm, at the end of reaction, the products produced by the photooxidation were analyzed by the VUV-PIMS and ATOFMS connected directly to the chamber using a Teflon line.

III. RESULTS AND DISCUSSION

A. Photoionization of gaseous products

The photoionization mass spectra of air and gaseous mixture before the photooxidation of toluene at the wavelength of 72.9 nm are shown in Fig.1. It is well known that air is made up of oxygen, nitrogen, and few water vapor, so it is not surprised that, the photoionization mass spectrum of air contains the mass peak m/z=18, 28, and 32. Compared with the photoionization mass spectrum of air, the photoionization mass spectrum of the gaseous mixture before the photooxidation of toluene, adds the mass peaks m/z=30, 46, 61, and 92. m/z=30 was assigned as the reagent NO, m/z=46 was assigned as NO_2, m/z=61 was assigned as methyl nitrate (CH_3ONO), and m/z=92 was assigned as toluene. So, no products are formed before the photooxidation.

Photoionization mass spectra of gaseous products formed from photooxidation of toluene at the wavelength of 72.9 nm are shown in Fig.2. Compared with the photoionization mass spectrum of gaseous mixture before the photooxidation of toluene, photoionization mass spectra of gaseous products add the mass peaks

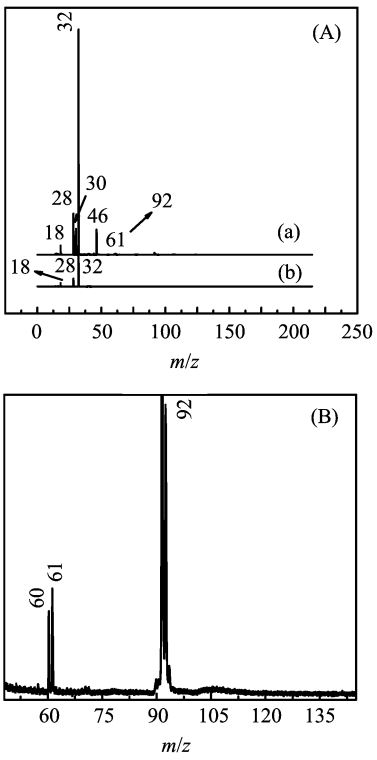

FIG. 1 (A) Photoionization mass spectra of gaseous mixture before the photooxidation of toluene (a) and air (b) at the wavelength of 72.9 nm. (B) Amplification mass spectrum from m/z=50 to m/z=140 of (a).

m/z=55, 64, 66, 72, 76, 78, 106, 108, and 122. It means that some products are formed after the photooxidation. Each ratio of mass to charge corresponds to a different compound molecule. Figure 3 gives the and molecular structures of speculated products from photooxidation of toluene with m/z=55, 66, and 76, which were assigned as hydrocarbons fragment ions of C_4H_7, C_5H_6, and C_6H_4, respectively [6, 7, 12]. The experimental results shows that in these molecules and radicals detected using PIMS, some are produced from H-atom abstraction from the methyl group of toluene and some from OH addition to the benzene ring in the toluene reaction. The chemical compositions identified in gas phase can also be divided into aromatic ring-retaining products (benzadehyde and cresol), non-aromatic ring-reserved products (2-methylfurane), and ring-opening carbonyl products (methyl glyoxal).

Most of the chemical compositions of photooxidation of toluene in our results are the same as those ones in Refs.[6, 7, 12]. However, previous smog chamber experiments only detect small amount of benzyl acid using GC-FID. It is difficult to distinguish benzyl acid existed in the photooxidation of toluene or produced via preparation of the examination sample. And our experimental results show that m/z=122 has the distinctly stronger intensities than m/z=106 and 108, indicating that yield of benzyl acid is higher than cresol and ben-

DOI:10.1088/1674-0068/24/06/672-678

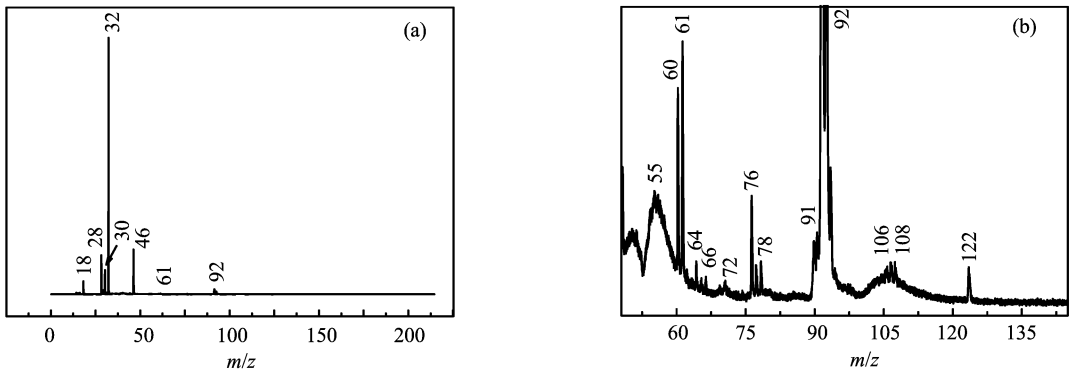

FIG. 2 (a) Photoionization mass spectra of gaseous products formed from photooxidation of toluene at the wavelength of 72.9 nm. (b) Amplification mass spectrum from m/z=50 to m/z=140 of (a).

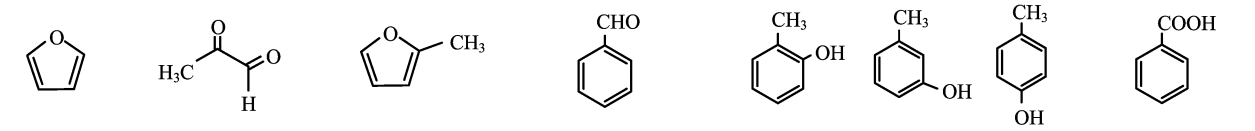

Furane [7]	Methylglyoxal [7]	2-methylfurane [7]	Benzaldehyde [6, 7, 12]	Cresol (*o*, *m*, *p*-isomers) [6, 7, 12]	Benzoic acid [7, 12]
m/z=64	m/z=72	m/z=78	m/z=106	m/z=108	m/z=122

FIG. 3 Molecular structures of speculated gaseous products from photooxidation of toluene.

zadehyde. This confirms that benzyl acid is the secondary product of the photooxidation of toluene. So, compared with the off-line methods, VUV-PIMS dose not need to prepare the examination sample, and can use as an on-line detector for atmospheric reactions simulated in smog chamber.

B. Laser desorption/ionization mass spectra of toluene SOA particles

According to the design principles on the measuring system of particle diameter, timing circuit, and laser desorption/ionization setup of ATOFMS. The time of flight mass spectroscopy is only obtained from those particles of secondary organic aerosol, whose diameter has been measured. The positive laser desorption/ionization mass spectra of SOA particles are shown in Fig.4. Each piece of mass spectrum corresponds to an aerosol particle, and the diameter and chemical composition might be different from each other.

A software compiled in Visual C++ was developed by our laboratory. Using this software, we can get the total number (N_0) of mass spectra of the experiment of toluene. Also, the number (n) of mass spectra including a defined ratio of m/z can be picked out from that N_0 of mass spectra. The ratio of n to N_0 is defined as η (η=n/N_0). For example, N_0=1302, and n=586 for mass spectra including m/z=58, η=45%. Figure 5 gives main mass spectra peaks, possible fragment ions, and the molecular structures of speculated products from photooxidation of toluene.

Photochemical oxidation of toluene is mainly initiated by hydroxyl radicals OH·. The OH-toluene reaction results in minor H-atom abstraction from the methyl group and major OH addition to the aromatic ring (about 90%) [22]. Under atmospheric conditions, the OH-toluene adduct reacts with O_2 to form oxygenated organic compounds or NO_x to yield nitrated organic compounds. These photooxidation products can also be divided into semivolatile organic compounds (furane, methylglyoxal, 2-methylfurane, benzaldehyde, cresol, and benzoic acid), nonvolatile organic compounds (2-hydroxyl-3-oxo-butanal, nitrotoluene, and methyl-nitrophenol). Nonvolatile organic compounds have very low vapor, which can only exist in the particle phase (Fig.5), and semivolatile, organic compounds can result in SOA formation through a self-nucleation process or the gas/particle partitioning on preexisting particulate matter [23], so it is not surprising to find that furane, methylglyoxal, 2-methylfurane, benzaldehyde, cresol, and benzoic acid are the predominant photooxidation products in both the gas phase and particle phase.

Possible mechanisms leading to the toluene photooxidation products are depicted in Fig.6 and Fig.7, and the rate constants of the key reations involved in the OH-intiated toluene photooxidation are list in Table I. The OH initiated photooxidation reaction pathway of abstraction/addition of toluene is depicted in Fig.6. Although H-abstraction leading to the formation of benzyl radical only estimated to be 10% of the OH-toluene reaction, the rate constant of benzyl radical with O_2 is higher than the OH-toluene adducts with O_2 (Table I).

DOI:10.1088/1674-0068/24/06/672-678

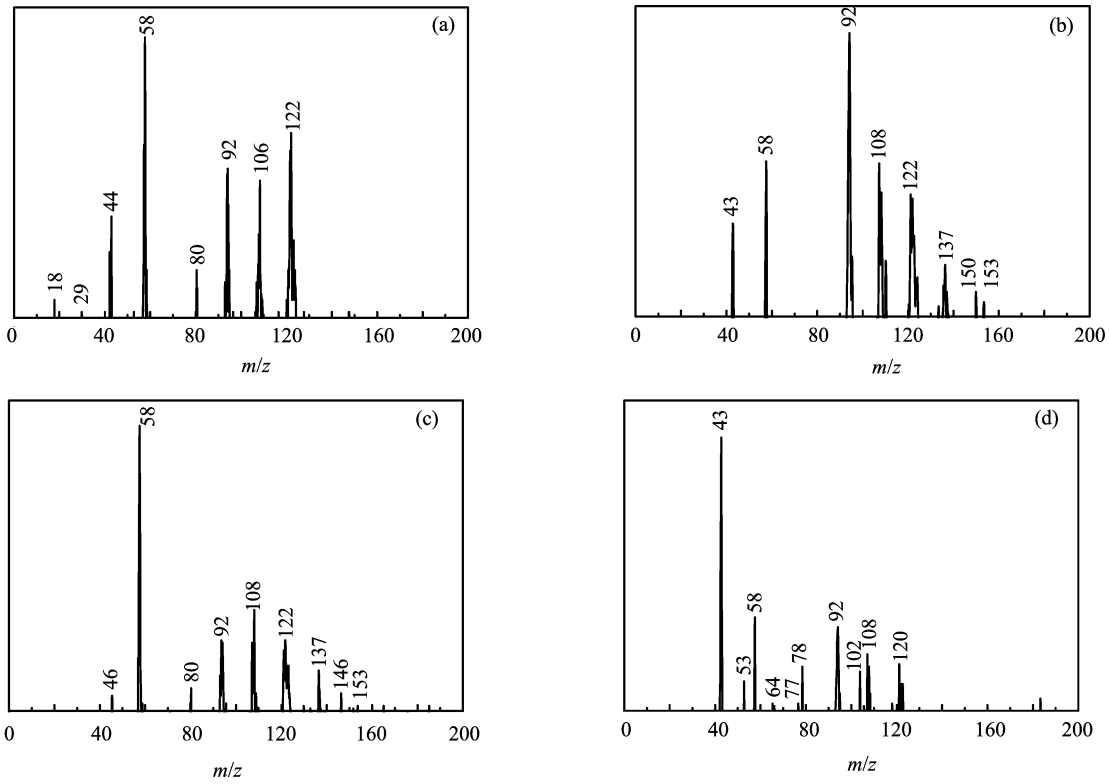

FIG. 4 Laser desorption/ionization time-of-flight mass spectra and four individual toluene SOA particles after 2 h photooxidation (aerosol diameter: (a) 1.40 μm, (b) 1.23 μm, (c) 0.98 μm, (d) 0.81 μm).

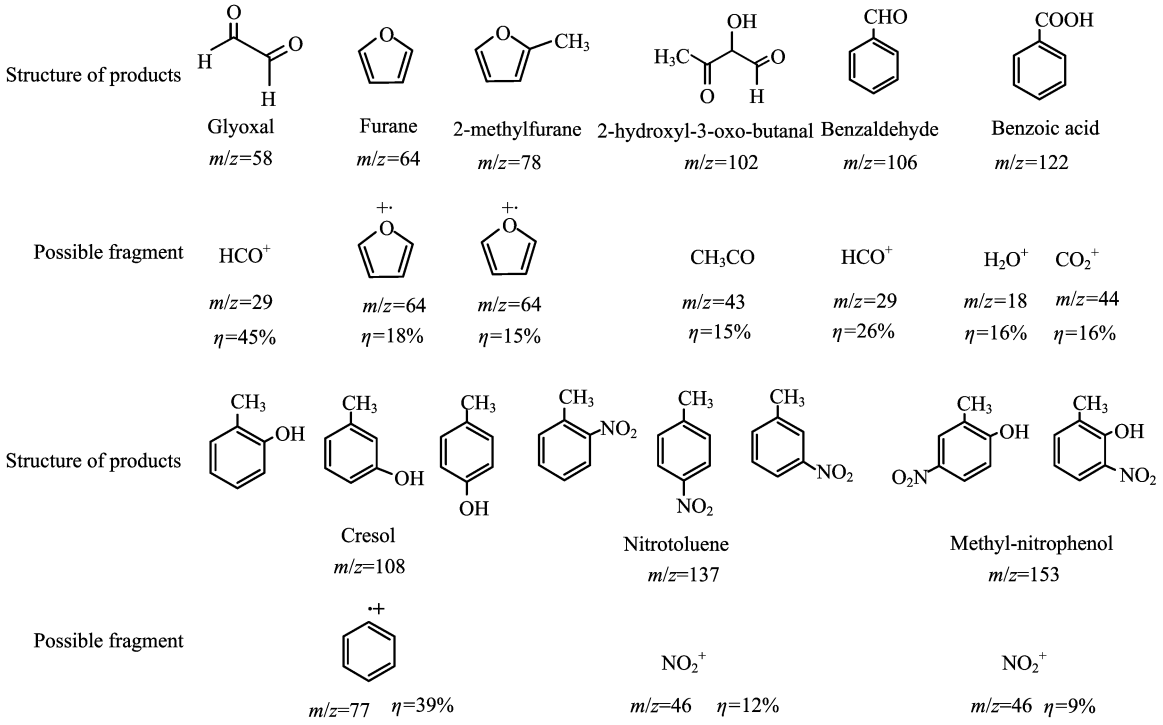

FIG. 5 Molecular structures of identified SOA products from photooxidation of toluene.

DOI:10.1088/1674-0068/24/06/672-678

TABLE I Rate constants of the key reations involved in the OH-intiated toluene photooxidation.

Reactants	Products	Rate constant/(cm^3/s)
Toluene+OH	OH-toluene adducts	1.0×10^{-11} [24]
Toluene+OH	Benzyl radical+H_2O	2.4×10^{-13} [25]
Benzyl radical+O_2	Benzyl peroxy radical	1.4×10^{-12} [26]
OH-toluene adducts+O_2	Peroxy radical	$(5-6)\times10^{-16}$ [27]
OH-toluene adducts+O_2	Cresol+HO_2	5.2×10^{-15} [28]
Peroxy radical+NO	Alkoxy radicals+NO_2	1.0×10^{-11} [29]

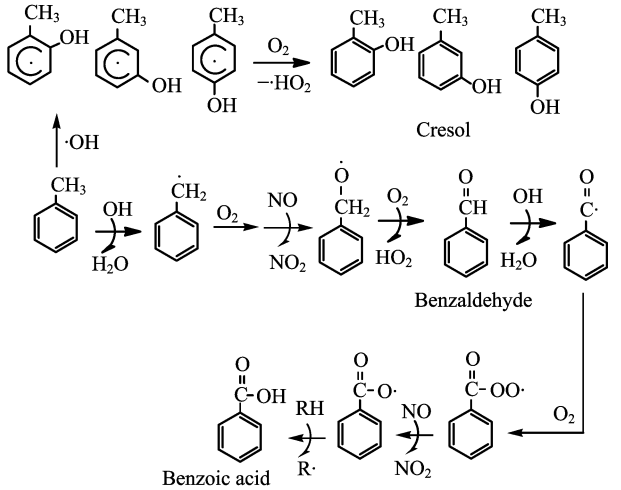

FIG. 6 Proposed reaction mechanisms leading to the formation of aromatic retaining products.

Oxygen adds to the benzyl radical to form benzyl peroxy radical. This peroxy radical can react with NO to form an alkoxy radical and NO_2. Oxygen can abstract a hydrogen atom from the alkoxy radical to form benzaldehyde, which can further react to form benzoic acid and to propagate the radical chain reaction [12].

As shown in Table I, the addition of OH to the ring results in methyl hydroxycyclohexadienyl radicals, a path estimated to be 90% of the OH-toluene reaction. Most products in toluene photooxidation result from subsequent reactions of the methyl hydroxycyclohexadienyl radical, comprising both ring-retaining species and ring-fragmentation species. As shown in Fig.6, OH can add to toluene in the *ortho*, *meta*, and *para* positions, with the ortho position energetically favored. Under atmospheric conditions, methyl hydroxycyclohexadienyl radicals react with O_2 either by O_2 addition to form peroxy radicals or by H-abstraction to yield cresol compounds. As the rate constant of H-abstraction is higher than O_2 addition, different cresol are the major products of the photooxidation of toluene [12]. And *ortho* methyl hydroxycyclohexadienyl radical through reaction with O_2 and NO, lead to the formation of alkoxy radicals [7]. Furane, methylglyoxal, 2-methylfurane can be produced through a bridged oxide intermediate on a bicyclosing from alkoxy radicals, which is shown in Fig.7.

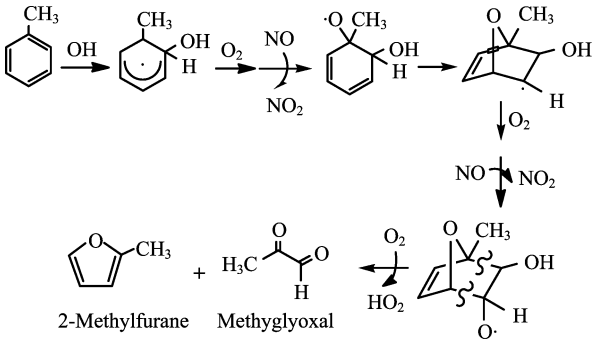

FIG. 7 Proposed reaction mechanisms leading to the formation of nonaromatic retaining products.

IV. CONCLUSION

The gaseous and particulate products from photooxidation of toluene in a smog chamber were investigated. Vacuum ultraviolet photoionization mass spectrometer using synchrotron radiation and aerosol time of flight mass spectrometer were employed to simultaneously detect the composition of the gaseous and particulate products, respectively. Furane, methylglyoxal, 2-methylfurane, benzaldehyde, cresol, and benzoic acid are the predominant photooxidation products in both the gas phase and particle phase. This will provide new information for discussing toluene photooxidation reaction mechanism.

V. ACKNOWLEDGMENTS

This work was supported by the Open Research Fund of Key Laboratory of Atmospheric Composition and Optical Radiation, Chinese Academy of Sciences (No.JJ-10-04), Knowledge Innovation Foundation of Chinese Academy of Sciences (KJCX2-YW-N24), and the National Natural Science Foundation of China (No.40975080 and No.10979061).

[1] M. A. Dearth, C. A. Glerczak, and W. O. Slegl, Environ. Sci. Technol. **26**, 1573 (1992).

DOI:10.1088/1674-0068/24/06/672-678

[2] T.Tanaka and T. Samukawa, Chemosphere **33**, 131 (1996).
[3] T. Etzkorn, B. Klotz, S. SØrensen, I. V. Partroescu, I. Barnes, K. H. Becker, and U. Platt, Atmos. Environ. **33**, 525 (1999).
[4] J. F. Pankow, Atmos. Environ. **28**, 188 (1994).
[5] J. R. Odum, T. P. W. Jungkamp, R. J. Griffin, R. C. Flagan, and J. H. Seinfeld, Science **276**, 96 (1997).
[6] J. Yu, H. E. Jeffries, and K. G. Sexton, Atmos. Environ. **31**, 2261 (1997).
[7] M. S. Jang and R. M. Kamens, Environ. Sci. Technol. **35**, 3626 (2001).
[8] C. Pilinis, S. N. Pandis, and J. H. Seinfeld, J. Geophys. Res. **100**, 18739 (1995).
[9] E. Annmarie, M. L. Susan, R. H. Jeffrey, J. H. Kevin, and R. C. Glen, Environ. Sci. Technol. **27**, 626 (1993).
[10] J. Schwartz, D. W. Dockery, and L. M. Neas, J. Air Waste Manage. Assoc. **46**, 927 (1996).
[11] V. Cocheo, P. Sacco, C. Boaretto, E. D. Saeger, P. P. Ballesta, H. Skov, E. Goelen, N. Gonzalez, and A. B. Caracena, Nature **404**, 141 (2000).
[12] H. J. L. Forstner, R. C. Flagan, and J. H. Seinfeld, Environ. Sci. Technol. **31**, 1345 (1997).
[13] M. Q. Huang, W. J. Zhang, L. Q. Hao, Z. Y. Wang, W. W. Zhao, X. J. Gu, X. Y. Guo, X. Y. Liu, B. Long, and L. Fang, J. Atmos. Chem. **58**, 237 (2007).
[14] D. T. Suess and K. A. Prather, Chem. Rev. **99**, 3007 (1999).
[15] E. Gloaguen, E. R. Mysak, S. R. Leone, M. Ahmed, and K. R. Wilson, Int. J. Mass. Spec. **258**, 74 (2006).
[16] K. Codling and R. P. Madden, J. Appl. Phys. **36**, 380 (1965).
[17] F. R. Elder, A. M. Gurewitsch, R. V. Langmuir, and H. C. Pollock, Phys. Rev. **71**, 829 (1947).
[18] Z. Y. Wang, L. Q. Hao, L. Z. Zhou, X. Y. Guo, W. W. Zhao, L. Fang, and W. J. Zhang, Sci. China B **49**, 267 (2006).
[19] Z. Y. Wang, L. Q. Hao, S. K. Zhou, B. Yang, C. Q. Huang, S. S. Wang, X. B. Shan, F. Qi, Y. W. Zhang, and L. S. Sheng, J. Mol. Struct.: THEOCHEM **826**, 192 (2007).
[20] X. Y. Liu, W. J. Zhang, Z. Y. Wang, M. Q. Huang, X. B. Yang, L. Tao, Y. Sun, Y. T. Xu, X. B. Shan, F. Y. Liu, and L. S. Sheng, J. Mass. Spectrom. **44**, 404 (2009).
[21] R. Atkinson, W. P. L. Carter, and A. M. Winer, J. Air Pollut. Control Assoc. **31**, 1090 (1981).
[22] R. Atkinson and J. Arey, Chem. Rev. **103**, 4605 (2003).
[23] J. R. Odum, T. P. W. Jungkamp, R. J. Griffin, H. J. L. Forstner, R. C. Flagan, and J. H. Seinfeld, Environ. Sci. Technol. **31**, 1890 (1997).
[24] I. Suh, D. Zhang, R. Zhang, L. T. Molina, and M. J. Molina, Chem. Phys. Lett. **364**, 454 (2002).
[25] V. H. Uc, J. R. Alvarez-Idaboy, A. Galano, I. Garca-Cruz, and A. Vivier-Bunge, J. Phys. Chem. A **110**, 10155 (2006).
[26] R. S. Karlsson, J. J. Szente, J. C. Ball, and M. M. Maricq, J. Phys. Chem. A **105**, 82 (2001).
[27] R. Knispel, R. Koch, M. Siese, and C. Zetzsch, Ber. Bunsen-Ges. Phys. Chem. **94**, 1375 (1990).
[28] M. Q. Huang, W. J. Zhang, Z. Y. Wang, L. Q. Hao, Z. Y. Wang, W. W. Zhao, X. Y. Liu, B. Long, and L. Fang, J. Mol. Struct.: THEOCHEM **862**, 28 (2008).
[29] I. Suh, R. Zhang, L. T. Molina, and M. J. Molina, J. Am. Chem. Soc. **125**, 12655 (2003).

DOI:10.1088/1674-0068/24/06/672-678